Rate-Determining Cooperative Effects of Bimolecular Reactions in Solution

Carlo Canepa*

Dipartimento di Chimica Generale ed Organica Applicata, Università di Torino, Corso Massimo d'Azeglio 48, 10125 Torino, Italy

Received: May 22, 2006; In Final Form: September 29, 2006

An expression for the rate constant of condensed-phase bimolecular reactions is derived. The key feature of the proposed model is the formulation of the energy-dependent rate constant in terms of the diffusion rate and the ratio of the volume in phase space that leads to product over the total volume. The dependence of the bimolecular rate constant by the reduced barrier $\bar{x} = E^{\ddagger}/kT$ is given in explicit form in terms of the incomplete and the complete gamma functions of Euler. The performance of the proposed model is tested against the experimental rate constants for the Menschutkin reaction by fitting the parameters of the expression for the rate constant to experimental data at various temperatures. The potential energy barrier obtained from the regression (16.75 kcal mol^{-1}) is close to the independently computed value at the CPCM B3LYP/CRENBL·6−311(+)G(d) level of theory (16.84 kcal mol^{-1}). The corresponding fitting to the transition state theory expression affords the lower value of 14.65 kcal mol^{-1}.

1. Introduction

In a previous work,[1] an expression for unimolecular rate constants was proposed to resolve the discrepancy between calculated potential energy barriers for enzyme-catalyzed reactions and the corresponding quantity obtained by an Eyring plot of the experimental rate constants at various temperatures. Wolfenden[2] places enthalpies of activation for a number of enzyme-catalyzed processes around 10−12 kcal mol^{-1}. The corresponding reactions in solvent exhibit a wider range of enthalpies of activation, corresponding to half-lives from 5 s to 10^9 years. On the other hand, quantum chemistry calculations on model enzyme systems fail to give potential energy reaction barriers below ∼20 kcal mol^{-1},[3] thus affording calculated rate constants based on the transition state theory (TST) many orders of magnitude below the observed values. This fact is a consequence of the exponential form of the rate constants given by TST, where the potential energy barrier only appears as an exponent. Alternatively, allowing efficient energy coupling between low-frequency protein vibrational modes to the reaction coordinate, one obtains a different form of the expression for the rate constant, namely

$$k_a(\bar{x}) = \nu \frac{z_v^{\ddagger}}{z_v} \frac{\Gamma(a,\bar{x})}{\Gamma(a)} \tag{1.1}$$

that is able to afford the observed rate constants for enzyme-catalyzed reactions with the intrinsic potential energy barriers computed ab initio. In eq 1.1 the quantities

$$\Gamma(a) = \int_0^{\infty} dx\, x^{a-1} e^{-x}$$

and

$$\Gamma(a,\bar{x}) = \int_{\bar{x}}^{\infty} dx\, x^{a-1} e^{-x}$$

are the complete and incomplete gamma functions of Euler, respectively. The system has a reduced barrier $\bar{x} = \beta E^{\ddagger}$, a number a of active modes energetically coupled, and crosses the reaction barrier with a frequency ν. The dependence of the rate constant of the potential energy is not purely exponential, and eq 1.1 predicts the curved Eyring plots observed by Stein[4] for chymotrypsin (Figure 1). The relationship between the number of active oscillators and the potential energy barrier was investigated for the hydrolysis of *N*-acetyl-L-tryptophan ethyl ester and *N*-acetyl-L-tyrosine ethyl ester catalyzed by α-chymotrypsin.[1] The frequency factors ν obtained are of the order $1 \div 10^3$ Hz, in agreement with the values given by Hammes[5] for individual rate constants converting various intermediates for the hydrolysis of an amide substrate.

Also, the effective coupling between modes in catalytic proteins was observed by Agarwal[6] through dynamic simulations. Excess energy was placed in a vibrational mode of the protein with a consequent increase of productive trajectories.

This work aims to naturally extend the model to bimolecular reactions in solution. The Menschutkin reaction (alkylation of amines) has been extensively studied both from the experimental and theoretical points of view. In particular, in a theoretical work,[7] rate constants were calculated according to TST making use of accurate partition functions for the condensed phase.[8] The regression of the experimental rate constants by Arnett[9] for the reaction of CH_3I with 3-bromopyridine in acetonitrile to the Eyring equation gives $\Delta H^{\ddagger} = 13.82$ kcal mol^{-1} and $\Delta S^{\ddagger} = -32.09$ cal mol^{-1} K^{-1}, respectively. The modified partition functions for the condensed phase afforded $\Delta S^{\ddagger} = -24.86$, but the calculated rate constant was 3 orders of magnitude lower than the observed value. This discrepancy is caused by a calculated barrier of 16.84 kcal mol^{-1} at the CPCM B3LYP/CRENBL·6-311(+)G(d) level of theory. In fact, a regression of the experimental rate constants to the TST expression

$$k_r(T) = \frac{kT}{h} \frac{q^{\ddagger}}{q^A q^B} e^{-\beta E^{\ddagger}} \tag{1.2}$$

with the partition functions corrected for the condensed phase

* To whom correspondence should be addressed. E-mail: carlo.canepa@unito.it.

10.1021/jp063120n CCC: $33.50
Published on Web 11/14/2006

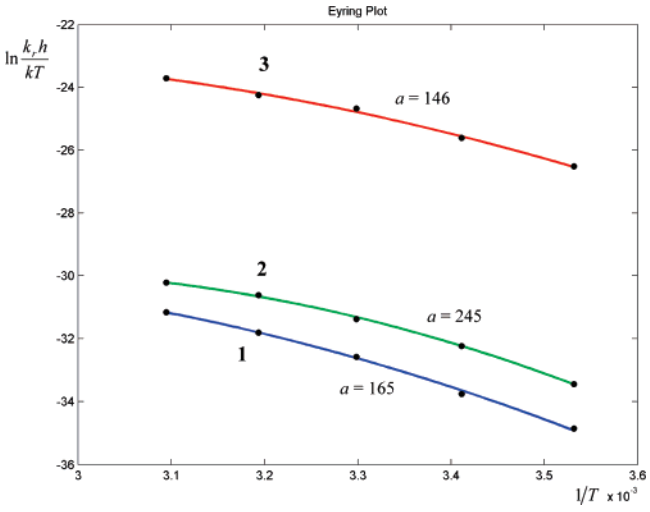

Figure 1. Experimental Eyring plots for the α-chymotrypsin-catalyzed hydrolysis of Suc-Phe-pNA (**1**), Suc-Ala-Phe-pNA (**2**), and Suc-Ala-Ala-Pro-Phe-pNA (**3**). The calculated quantity $\ln(hk_r/kT)$ is plotted versus $1/T$ (curves), with the rate constant given by the expression $k_r = \tilde{\nu}\Gamma(a,\bar{x})/\Gamma(a)$ ($\tilde{\nu} = \nu z_\nu^\ddagger/z_\nu$ in eq 1.1).

(the values of q, partition functions per unit volume are reported in Table 1) yields a potential energy barrier of 14.65 kcal mol^{-1}.

2. Statistical Model for Bimolecular Reactions in the Condensed Phase

Two species A and B with total energy E collide with formation of a vibrationally excited species C*, which in turn can revert back to reactants or evolve to products P with the unimolecular rate constants k_{-1} and k_2 (Scheme 1).

SCHEME 1

$$A + B \underset{k_{-1}}{\overset{k_d}{\rightleftharpoons}} C^* \xrightarrow{k_2} P$$

The steady-state approximation for C* gives the energy-dependent rate constant

$$k(E) = \frac{k_d k_2}{k_{-1} + k_2} \tag{2.1}$$

The elementary energy-dependent rate constant k_2 is the product of the fundamental frequency ν_2 and the ratio of phase-space volume leading to product and the total volume

$$k_2 = \nu_2 \frac{\rho^\ddagger(E,E^\ddagger)\,\mathrm{d}E}{\rho(E)\,\mathrm{d}E + \rho^\ddagger(E,E^\ddagger)\,\mathrm{d}E} \tag{2.2a}$$

and

$$k_{-1} = \nu_{-1}\left[1 - \frac{\rho^\ddagger(E,E^\ddagger)\,\mathrm{d}E}{\rho(E)\,\mathrm{d}E + \rho^\ddagger(E,E^\ddagger)\,\mathrm{d}E}\right] \tag{2.2b}$$

In eqs 2.2a−b $\rho^\ddagger(E, E^\ddagger)$ represents the density of states of the transition structure, whereas $\rho(E)$ is that of the corresponding reactant species. The frequency ν_2 includes the rotational motion of the reactant molecules leading to the interaction (via vibrational degrees of freedom) in the direction of the reaction coordinate forming the transition structure. The unimolecular rate constants k_2 and k_{-1} are expressed as the fraction of the volume of phase space of the system C* (with s vibrational modes and a active modes) that leads to products or reactants, respectively, multiplied by the intrinsic response frequencies ν_{-1} and ν_2.[10] Within this formulation, the energy-dependent rate constant is given by

$$k(E,E^\ddagger) = \frac{k_d(E)}{\eta\dfrac{\rho(E)}{\rho^\ddagger(E,E^\ddagger)} + 1} \tag{2.3}$$

with $\eta = \nu_{-1}/\nu_2$. It is convenient to express quantities that depend on energy and temperature in terms of the reduced energy $x = \beta E$ and the reduced barrier $\bar{x} = \beta E^\ddagger$, with $\beta = (kT)^{-1}$. The energy-dependent rate constant is thus the product of the diffusion rate constant k_d and the probability of having energy in excess of the reduced potential energy barrier $\bar{x}$ in a active modes

$$P(x) = \frac{k_2}{k_{-1} + k_2} = \frac{\rho^\ddagger(x,\bar{x})}{\eta\rho(x) + \rho^\ddagger(x,\bar{x})} = \left(\frac{\eta\rho(x)}{\rho^\ddagger(x,\bar{x})} + 1\right)^{-1} \tag{2.4}$$

The quantity $\rho^\ddagger(x,\bar{x})$ may be derived as follows. The joint density of states with energy between $E^\ddagger$ and E in a active modes is

$$\rho^\ddagger(E;E^\ddagger) = \int_{E^\ddagger}^{E} \mathrm{d}\epsilon\ \rho_a(\epsilon)\rho_{s-a}(E-\epsilon)$$

Using the classical form for the density of states, we have

$$\rho^\ddagger(E,E^\ddagger) = \int_{E^\ddagger}^{E} \mathrm{d}\epsilon \frac{\epsilon^{a-1}}{(a-1)!\prod_{i=1}^{a} h\nu_i^\ddagger} \frac{(E-\epsilon)^{s-a-1}}{(s-a-1)!\prod_{i=a+1}^{s} h\nu_i^\ddagger}$$

$$= \frac{1}{\prod_{i=1}^{s} h\nu_i^\ddagger\,\Gamma(a)\,\Gamma(s-a)} \int_{E^\ddagger}^{E} \mathrm{d}\epsilon\ \epsilon^{a-1}(E-\epsilon)^{s-a-1}$$

Changing the variable to $u = \epsilon/E$, we get

$$\rho^\ddagger(x,\bar{x}) = \prod_{i=1}^{s}\frac{kT}{h\nu_i^\ddagger}\frac{x^{s-1}}{\Gamma(a)\Gamma(s-a)}\frac{1}{kT}\int_{\bar{x}/x}^{1} \mathrm{d}u\ u^{a-1}(1-u)^{s-a-1}$$

The classical vibrational partition function is

$$z_\nu = \int_0^\infty \mathrm{d}t \frac{t^{s-1}}{\Gamma(s)}\prod_{i=1}^{s}\frac{kT}{h\nu_i}e^{-t} = \prod_{i=1}^{s}\frac{kT}{h\nu_i} \tag{2.5}$$

so we have

$$\rho^\ddagger(x,\bar{x}) = \frac{\beta z_\nu^\ddagger x^{s-1}}{\Gamma(a)\Gamma(s-a)}\int_{\bar{x}/x}^{1} \mathrm{d}u\ u^{a-1}(1-u)^{s-a-1}$$

The integral may be expressed in terms of the complete and incomplete beta functions of Euler

$$\int_{\bar{x}/x}^{1} \mathrm{d}u\ u^{a-1}(1-u)^{s-a-1} = \mathrm{B}(a,s-a) - \mathrm{B}(a,s-a;\bar{x}/x)$$

The joint density of states may thus be written as

$$\rho^\ddagger(x,\bar{x}) = \frac{\beta z_\nu^\ddagger x^{s-1}}{\Gamma(s)}\left[1 - \frac{\mathrm{B}(a,s-a;\bar{x}/x)}{\mathrm{B}(a,s-a)}\right] \tag{2.6}$$

The quantity in brackets was already defined in a previous work[11] as $\psi_a(x,\bar{x})$. For s and a integers it may be integrated by

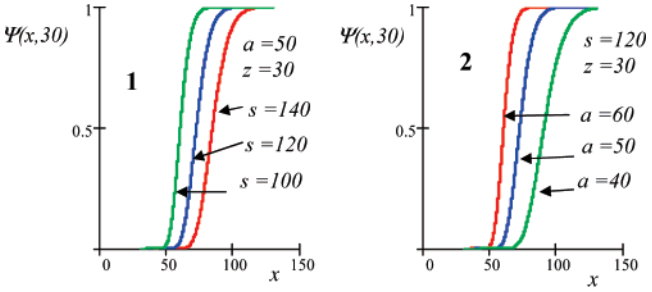

Figure 2. Plots of the function $\Psi(x,z)$ with various values of the parameters s (**1**) and a (**2**).

parts to give

$$\psi_a(x,\bar{x}) = \sum_{i=0}^{a-1}\binom{s-1}{i}\left(\frac{\bar{x}}{x}\right)^i\left(1-\frac{\bar{x}}{x}\right)^{s-1-i} \tag{2.7}$$

When the number of active modes is one, eq 2.7 reduces to the classical expression $\psi_1(x,\bar{x}) = (1-\bar{x}/x)^{s-1}$. Plots of the function ψ are shown in Figure 2 for different values of the parameters s and a. With the density of states 2.6, we may express the ratio of volumes in phase space as

$$\frac{\rho^{\ddagger}(x,\bar{x})}{\rho(x)} = \frac{z_v^{\ddagger}}{z_v}\psi_a(x,\bar{x}) \tag{2.8}$$

Consequently, the probability of reaction is

$$P(x) = \left(\frac{z_v}{z_v^{\ddagger}}\frac{\eta}{\psi_a} + 1\right)^{-1} \tag{2.9}$$

The rate constant is given by the thermodynamic average of $k_d(x)$ $P(x)$

$$k_r(\bar{x}) = \int_{\bar{x}}^{\infty} dx\, k_d(x)\left(\frac{z_v}{z_v^{\ddagger}}\frac{\eta}{\psi_a} + 1\right)^{-1}\frac{\rho(x)}{z_v}e^{-x} \tag{2.10}$$

With the density of vibrational states of the cluster C* taken as the classical expression eq 2.10 then takes the general form

$$\rho(x) = \frac{\beta z_v}{\Gamma(s)}x^{s-1} \tag{2.11}$$

$$k_r(\bar{x}) = \frac{1}{\Gamma(s)}\int_{\bar{x}}^{\infty} dx\, k_d(x)\left(\frac{z_v}{z_v^{\ddagger}}\frac{\eta}{\psi_a} + 1\right)^{-1} x^{s-1}e^{-x} \tag{2.12}$$

Expression 2.12 may be evaluated numerically, once an expression for $k_d(x)$ is provided. In this work, we consider reactions that are not diffusion-limited and neglect the dependence of the diffusion rate constant k_d on the energy. Since both the ratio $z_v/z_v^{\ddagger}$ and η are of the order 10^3,[10] and $\psi_a(x,z) \leq 1$, we may safely neglect 1 in parentheses in 2.12 to get

$$k_r(\bar{x}) = \frac{k_d}{\eta}\frac{z_v^{\ddagger}}{z_v}\frac{1}{\Gamma(s)}\int_{\bar{x}}^{\infty} dx\, \psi_a x^{s-1}e^{-x} \tag{2.13}$$

Using the equality

$$\frac{1}{\Gamma(s)}\int_z^{\infty} dx\, \psi_a(x,z)x^{s-1}e^{-x} = \frac{1}{\Gamma(a)}\int_z^{\infty} dx\, x^{a-1}e^{-x} \tag{2.14}$$

which is proven in the appendix, we have the final form

$$k_r(\bar{x}) = \frac{k_d}{\eta}\frac{z_v^{\ddagger}}{z_v}\frac{\Gamma(a,\bar{x})}{\Gamma(a)} \tag{2.15}$$

Remarkably, equality 2.14 states that the thermal-averaged rate constant is independent of the total number of coordinates s, but it is only dependent on the number a of coordinates coupled to the reaction. Plots of the ratio $\Gamma(a,\bar{x})/\Gamma(a)$ are shown in Figure 3 as functions of a and $\bar{x}$. For $a > 1$ this function significantly differs from the exponential $e^{-\bar{x}}$. In particular, there is a domain of $\bar{x}$ where the first derivative is close to zero and $k_r(\bar{x})$ does not change significantly varying $\bar{x}$.

3. Methods of Calculation

Quantum chemistry calculations were carried out using the Gaussian 98 suite of programs,[12] utilizing redundant internal coordinates geometry optimization.[13] All structures were fully optimized at the B3LYP[14] level of theory. The CRENBL[15] basis set was used for the iodine atom and the 6-311G(d) for the other atoms of the substrates CH_3I and 3-bromopyridine. A set of diffuse functions with exponent 0.0639 was also added to the nitrogen atom of pyridine. This combination of basis sets is designated CRENBL·6-311(+)G(d). Solvation calculations based on continuum models were carried out with the polarizable conductor (CPCM) method.[16] Vibrational frequency calculations were used to characterize the stationary points as either minima or first-order saddle points at the level indicated. Molecular graphics were obtained with the program Moldraw.[17] The partition functions were evaluated at various temperatures and 1 bar making use of a model where the rotational contribution is formulated for the condensed phase.[8] The vibrational contribution of the partition functions was calculated within the harmonic oscillator approximation.[18]

4. Computational Results

The structures of the intermediate reactant cluster (**1**) and the corresponding transition structure (TS-**2**) for the reaction of 3-bromopyridine and iodomethane in acetonitrile, optimized at the CPCM B3LYP/CRENBL·6-311(+)G(d) level of theory, are reported in Figure 4. For these structures and isolated reactants, both the ratio of the vibrational partition function of the transition structure to the reactant cluster ($z_v^{\ddagger}/z_v$, used in eq 2.15) and the corresponding ratio of partition functions per unit volume ($q^{\ddagger}/q^A q^B$, used in eq 1.2) were computed at the same level of theory at the experimental temperatures, and are reported in Table 1.

With these data, an unconstrained nonlinear regression of experimental rate constants for the methylation of 3-bromopyridine to eq 2.15 was performed with the Levenberg−Marquardt algorithm[19] and the resulting plot is reported in Figure 5. Analogous regressions were performed on the same set of data making use of eq 1.2, and the relative standard deviations (σ) from the n experimental points $\bar{k}(T_i)$

$$\sigma = \sqrt{\frac{1}{n}\sum_{i=1}^{n}\left[1-\frac{\bar{k}(T_i)}{k_r(T_i)}\right]^2}$$

are reported in Table 2. The regression optimized the relevant parameters, i.e., $E^{\ddagger}$ in eq 1.2, and both k_d/η and $E^{\ddagger}$ in eq 2.15.

Notwithstanding the fact that the proposed model in its present form lacks the ability to compute rate constants from first principles, a regression to expression 2.15 affords a potential

TABLE 1: Ratios of Condensed-Phase Total Partition Functions per Unit Volume and Their Vibrational Contributions for the Structures CH_3I (q^A), 3-bromopyridine (q^B), Cluster (q^{cl}), and TS ($z^{\ddagger}$, $q^{\ddagger}$)[a]

T/K	273.88	283.95	293.95	303.87
$(q^{\ddagger}/q^A q^B)N$	4.0154×10^{-10}	3.9502×10^{-10}	3.8853×10^{-10}	3.8225×10^{-10}
$z_v^{\ddagger}/z_v^{cl}$	9.1182×10^{-5}	9.0318×10^{-5}	8.9420×10^{-5}	8.8500×10^{-5}
k_r/L mol^{-1} s^{-1}[b]	5.11×10^{-6}	1.35×10^{-5}	3.12×10^{-5}	7.00×10^{-5}
k_r/L mol^{-1} s^{-1}[c]	4.69×10^{-6}	1.24×10^{-5}	3.06×10^{-5}	7.05×10^{-5}
k_r/L mol^{-1} s^{-1}[d]	5.14×10^{-6}	1.32×10^{-5}	3.14×10^{-5}	6.99×10^{-5}

[a] The calculations are at the CPCM B3LYP/CRENBL·6-311(+)G(d) level of theory at various temperatures. The experimental and the computed bimolecular rate constants for the reaction of CH_3I and 3-bromopyridine in acetonitrile are also reported. [b] Experimental from Arnett, E. M.; Reich, R. *J. Am. Chem. Soc.* **1980**, *102*, 5892−5902. [c] Calculated from eq 1.2 with $E^{\ddagger} = 14.65$ kcal mol^{-1}. [d] Calculated from eq 2.15 with $k_d/\eta = 1.77 \times 10^5$ L mol^{-1} s^{-1} and $E^{\ddagger} = 16.75$ kcal mol^{-1}.

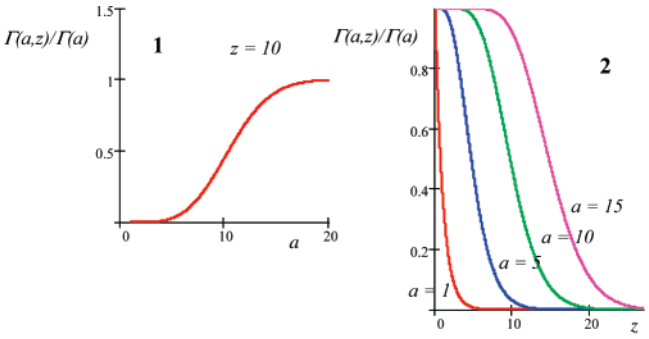

Figure 3. Plots of the expression $\Gamma(a,z)/\Gamma(a)$ as a function of a (**1**) and z (**2**).

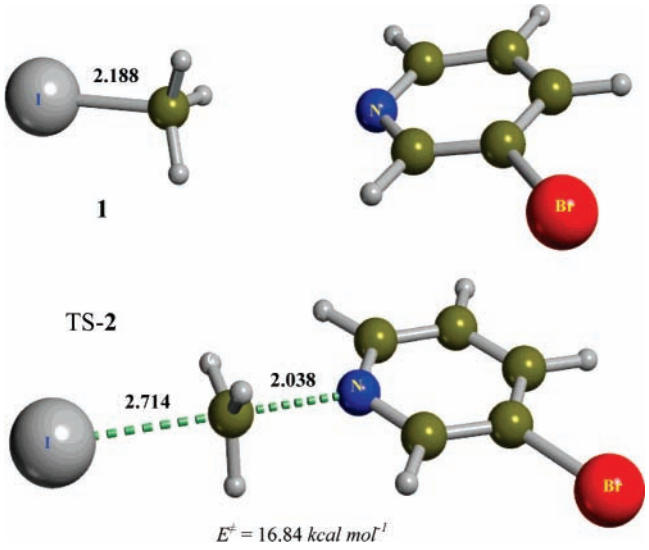

Figure 4. Structures and potential energy barrier ($E^{\ddagger}$) for the intermediate cluster and transition structure for the alkylation of 3-bromopyridine by iodomethane in acetonitrile at the CPCM B3LYP/CRENBL·6-311(+)G(d) level of theory. Geometries are fully optimized, and distances are in angstroms.

energy barrier for the Menschutkin reaction in Figure 4 of 16.75 kcal mol^{-1}, very close to the corresponding barrier computed at the CPCM B3LYP/CRENBL·6-311(+)G(d) level of theory (16.84 kcal mol^{-1}). This fact, and the ability to predict the curved Eyring plots in Figure 1, strongly support eqs 1.1 and 2.15 for the unimolecular and bimolecular rate constants, respectively. On the other hand, the regression of experimental rate constants to eq 1.2 (Table 2) affords a lower potential energy barrier (14.65 kcal mol^{-1}) with respect to the DFT value.

The estimated[20] value of the ratio η is about 2 orders of magnitude higher than that already found for gas-phase reactions.[10] The condensed phase is thus more efficient in deactivating the intermediate cluster C* in Scheme 1 with respect to the gas phase.

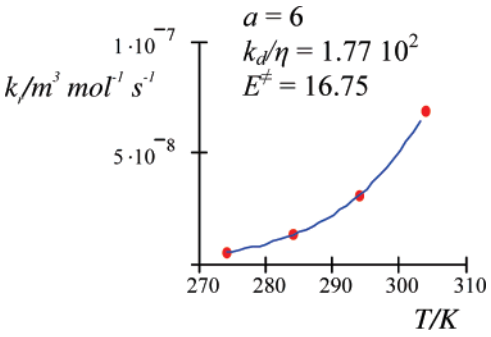

Figure 5. Regressions of the experimental rate constants for the reaction of CH_3I with 3-bromopyridine in acetonitrile. The dots represent experimental points and the curve a plot of eq 2.15 for the indicated values of the parameters a, k_d/η (m^3 mol^{-1} s^{-1}), and $E^{\ddagger}$ (potential energy barrier, kcal mol^{-1}).

TABLE 2: Parameters for the Various Expressions in the Text Giving the Rate Constant as a Function of Temperature[a]

eq	pre-exp	$E^{\ddagger}$	σ
1.2	2.397×10^3	14.65	5.863×10^{-2}
2.15	8.397×10^4	16.75	1.201×10^{-2}

[a] All parameters were obtained by regressions to the experimental rate constants for the reaction CH_3I and 3-bromopyridine in acetonitrile. Partition functions are calculated at the CPCM B3LYP/CRENBL·6-311(+)G(d) level of theory (at the same level of theory the corresponding barrier is 16.84 kcal mol^{-1}).

The six coupled modes a obtained by the fitting of eq 2.15 to the experimental rate constants are considerably less than what has been obtained in the case on enzyme catalysis. This fact may be explained by the more disordered structure of a solvent with respect to the specific active site of an enzyme, but this dynamical effect reflects the substantial participation of the solvent in determining the reaction rate.

5. Conclusions

1. The elementary rate constants of a bimolecular encounter (for the association to an intermediate cluster and dissociation to reactants and products) are expressed in terms of their diffusion coefficients and the density of vibrational states of the cluster and transition structure.

2. The energy-dependent rate constant is in turn formulated in terms of the diffusion rate constants and the fundamental probability $(z_v/z_v^{\ddagger}\psi_a + 1)^{-1}$, the ratio of the volume in phase space leading to products over the total volume. The thermodynamic average of the energy-dependent rate constant affords the final expression for the thermal-averaged rate constant.

3. The proposed functional form of the rate constant is fitted to the corresponding experimental values of a well studied process and the temperature dependence of the experimental data is well reproduced.

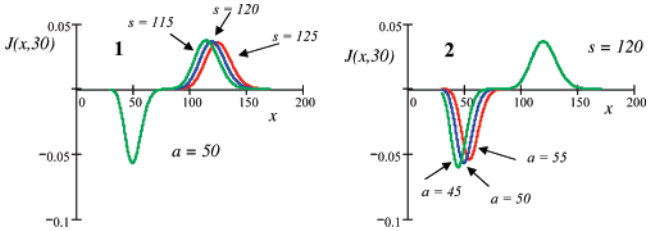

Figure 6. Plots of the function $J(x,z)$ with various values of the parameters s (**1**) and a (**2**).

4. The number of active modes that minimizes the relative standard deviation from the experimental rate constants is found to be considerably lower than that found for enzyme-catalyzed reactions. This difference is attributed to the short-range structure of liquids, as opposite to the optimal structure of enzymes.

6. Appendix. Proof of Theorem 2.14

First, we consider the left-hand side of eq 2.14 as a function $f(z)$. Its first derivative with respect to z is given by

$$f'(z) = \frac{1}{\Gamma(s)}\int_z^\infty dx\, \frac{\partial \psi_a}{\partial z}(x,z)x^{s-1}e^{-x} - \frac{1}{\Gamma(s)}\psi_a(z,z)z^{s-1}e^{-z} \tag{6.1}$$

The second term on the right-hand side of eq 6.1 is equal to zero since it follows from 2.6 that $\psi_a(z,z) = 0$. The first derivative of $\psi_a(x,z)$ is given by

$$\frac{\partial \psi_a}{\partial z}(x,z) = -\frac{\Gamma(s)}{\Gamma(a)\Gamma(s-a)}\frac{1}{x}\left(\frac{z}{x}\right)^{a-1}\left(1-\frac{z}{x}\right)^{s-a-1} \tag{6.2}$$

Substituting 6.2 in 6.1 we have

$$f'(z) = \frac{1}{\Gamma(s)}\int_z^\infty dx \left(-\frac{\Gamma(s)}{\Gamma(a)\,\Gamma(s-a)}\frac{1}{x}\left(\frac{z}{x}\right)^{a-1}\left(1-\frac{z}{x}\right)^{s-a-1}\right)x^{s-1}e^{-x}$$

that simplifies to

$$f'(z) = -\frac{z^{a-1}}{\Gamma(a)\,\Gamma(s-a)}\int_z^\infty dx\,(x-z)^{s-a-1}e^{-x}$$

Changing the variable of integration to $u = x - z$, we obtain

$$f'(z) = -\frac{z^{a-1}}{\Gamma(a)\,\Gamma(s-a)}\int_0^\infty du\, u^{s-a-1}e^{-(z+u)} = -\frac{z^{a-1}e^{-z}}{\Gamma(a)} \tag{6.3}$$

The right-hand side of eq 2.14 is also a function g of z, and its first derivative is given by

$$g'(z) = -\frac{z^{a-1}e^{-z}}{\Gamma(a)} \tag{6.4}$$

We have thus shown that the derivatives with respect to z of both sides of 2.14 are equal. Consequently, the functions $f(z)$ and $g(z)$ differ at most by a constant

$$f(z) = g(z) + C$$

To find the value of C, we observe that, for $z = 0$, eq 2.14 gives $f(0) = g(0) = 1$, and that implies $C = 0$. This completes the proof. The equality 2.14 may be equivalently stated defining the function

$$J(x,z) = \psi_a(x,z)\frac{x^{s-1}}{\Gamma(s)}e^{-x} - \frac{x^{a-1}}{\Gamma(a)}e^{-x} \tag{6.5}$$

and its property

$$\int_z^\infty dx\, J(x,z) = 0 \tag{6.6}$$

The behavior of $J(x,z)$ is plotted in Figure 6.

References and Notes

(1) Canepa, C. *J. Phys. Chem. B* **2003**, *107*, 4437−4443.
(2) Wolfenden, R.; Snider, M. J. *Acc. Chem. Res.* **2001**, *34*, 938−945.
(3) (a) Bach, R. D.; Canepa, C. *J. Am. Chem. Soc.* **1997**, *119*, 11733. (b) Bach, R. D.; Canepa, C.; Glukhovtsev, M. N. *J. Am. Chem. Soc.* **1999**, *121*, 6555.
(4) Stein, R. L.; Case, A. *Biochemistry* **2003**, *42*, 3335−3348.
(5) Hammes, G. G. *Biochemistry* **2002**, *41*, 8221−8228.
(6) Agarwal, P. K. *J. Am. Chem. Soc.* **2005**, *127*, 15248−15256.
(7) Canepa, C.; Mosso, M.; Maranzana, A.; Tonachini, G. *Eur. J. Org. Chem.* **2005**, *15*, 3342−3347.
(8) Canepa, C. *J. Chem. Phys.* **2001**, *115*, 7592−7598.
(9) Arnett, E. M.; Reich, R. *J. Am. Chem. Soc.* **1980**, *102*, 5892−5902.
(10) Canepa, C. *Int. J. Chem. Kinet.* **2005**, *37*, 233−242.
(11) Canepa, C.; Bach, R. D. *Phys. Chem. Chem. Phys.* **2001**, *3*, 4072.
(12) Frisch, M. J.; Trucks, G. W.; Schlegel, H. B.; Scuseria, G. E.; Robb, M. A.; Cheeseman, J. R.; Zakrzewski, V. G.; Montgomery, J. A., Jr.; Stratmann, R. E.; Burant, J. C.; Dapprich, S.; Millam, J. M.; Daniels, A. D.; Kudin, K. N.; Strain, M. C.; Farkas, O.; Tomasi, J.; Barone, V.; Cossi, M.; Cammi, R.; Mennucci, B.; Pomelli, C.; Adamo, C.; Clifford, S.; Ochterski, J.; Petersson, G. A.; Ayala, P. Y.; Cui, Q.; Morokuma, K.; Malick, D. K.; Rabuck, A. D.; Raghavachari, K.; Foresman, J. B.; Cioslowski, J.; Ortiz, J. V.; Stefanov, B. B.; Liu, G.; Liashenko, A.; Piskorz, P.; Komaromi, I.; Gomperts, R.; Martin, R. L.; Fox, D. J.; Keith, T.; Al-Laham, M. A.; Peng, C. Y.; Nanayakkara, A.; Gonzalez, C.; Challacombe, M.; Gill, P. M. W.; Johnson, B. G.; Chen, W.; Wong, M. W.; Andres, J. L.; Head-Gordon, M.; Replogle, E. S.; Pople, J. A. *Gaussian 98*; Gaussian, Inc.: Pittsburgh, PA, 1998.
(13) Peng, C.; Ayala, P. Y.; Schlegel, H. B.; Frisch, M. J. *J. Comput. Chem.* **1996**, *17*, 49.
(14) (a) Becke, A. D. *J. Chem. Phys.* **1993**, *98*, 5648. (b) Stevens, P. J.; Devlin, F. J.; Chablowski, C. F.; Frisch, M. J. *J. Phys. Chem.* **1994**, *80*, 11623.
(15) Hurley, M. M. *J. Chem. Phys.* **1986**, *84*, 6840−6853.
(16) Barone, V.; Cossi, M. *J. Phys. Chem. A* **1998**, *102*, 1995−2001.
(17) (a) Ugliengo, P.; Viterbo, D.; Borzani, G. *J. Appl. Crystallogr.* **1988**, *21*, 75. (b) Ugliengo, P.; Borzani, G.; Viterbo, D. *Z. Crystallogr.* **1988**, *185*, 712. (c) Ugliengo, P.; Viterbo, D.; Chiari, G. *Z. Crystallogr.* **1993**, *207*, 9.
(18) McQuarrie, D. A. In *Statistical Thermodynamics*; University Science Books: Mill Valley, CA, 1973.
(19) Press, W. H.; Flannery, W. T.; Teukolsky, S. A.; Vetterling, B. P. In *Numerical Recipes in C*; Cambridge University Press: New York, 1992.
(20) The rate constant for the diffusion process k_d may be estimated according to the model of Smoluchwski (for details, see Steinfeld, J. I.; Francisco, J. S.; Hase, W. L. In *Chemical Kinetics and Dynamics*; Prentice Hall: Englewood Cliffs, NJ, 1989). The expression $k_d = 4\pi(D_A + D_B)(r_A + r_B)$ makes use of the molecular radii ($r_A = 3.90 \times 10^{-10}$, $r_B = 4.54 \times 10^{-10}$ *m* for CH_3I and 3-bromopyridine at the B3LYP/CRENBL·6-311-(+)G(d) level of theory). The diffusion coefficients for CH_3I and 3-bromopyridine in acetonitrile may be estimated according to the Stokes−Einstein expression $D_i = kT/6\pi\gamma r_i$, with the experimental viscosity coefficients γ. The values $D_A = 1.52 \times 10^{-9}$ and $D_B = 1.30 \times 10^{-9}$ m^2 s^{-1} afford a diffusion rate constant of 1.80×10^{10} L mol^{-1} s^{-1}, which in turn gives $\eta = 1.02 \times 10^5$.